DOI: https://doi.org/10.46354/i3m.2019.mas.005

OPTIMAL HYBRID DRIVE SYSTEM ARCHITECTURE EXPLORATION CONSIDERING PERFORMANCE INDEX OF 48V MILD HEV

Yonghyeok Ji[(a)], Taeho Park[(b), (c)], Hyeongcheol Lee*[(d)]

[(a),(b)]Department of Electrical Engineering, Hanyang University, 222, Wangsimni-ro, Seongdong-gu, Seoul 133-791, Korea
[(c)]Green Car Power System R&D Division, Korea Automotive Technology Institute, 303 Pungse-ro, Pungse-myeon, Dongnam-gu, Cheonan-si, Chungnam 31214, Korea
[(d)]Department of Electrical and Biomedical Engineering, Hanyang University, 222, Wangsimni-ro, Seongdong-gu, Seoul 133-791, Korea

[(a)]youg0839@hanyang.ac.kr, [(b), (c)]koreapow@hanyang.ac.kr, [(d)]hclee@hanyang.ac.kr
*Corresponding Author hclee@hanyang.ac.kr

ABSTRACT
The 48V hybrid system has mostly adopted parallel hybrid system architecture. In the parallel hybrid system, various architecture can be derived depending on the location of the motor. In this paper, we explored a hybrid system architecture considering one or two motors and 48V electric supercharger and derived the optimal architecture by comparing the performance of each architecture. Performance of the hybrid system is mostly evaluated as fuel economy. However, since the hybrid system has increasingly been applied to various types of vehicles with different purpose of the operation, another performance index for evaluating a hybrid system is needed. Therefore, in this paper, we introduced an additional performance index to evaluate the hybrid electric drive system and used it to derive the optimal architecture of the hybrid electric drive system. We used *Dynamic programming (DP)* to evaluate each architecture and *DP* simulation was performed in the Matlab environment.

Keywords: 48V mild hybrid system, HEV architecture, *Dynamic programming*, Performance index

1. INTRODUCTION

As fuel economy and emission gas regulations are strengthened globally, environmentally friendly vehicles of various types (BEV, FCEV, (P)HEV, etc.) are being introduced to the market. However, due to the problem of the high-cost electric drive system or charging infrastructure, it is still difficult for vehicles to replace the demand for existing internal combustion engine vehicles. According to this trend, a mild hybrid system based on a 48V power supply has recently attracted attention as a new alternative and many kinds of research about 48V mild hybrid system are being conducted. (Malte Kuypers 2014; Mark Schudeleit and Christian Sieg 2015; Anthony Rick and Brain Sisk 2015; Andreas Baumgardt and Dieter Gerling 2015a,b; Anthony Rick and Brain Sisk 2015; Zifan Liu and Andrej Ivanco 2016; Junyong Park and Taeho Park 2017)

There are various hybrid drive system architectures according to the arrangement of the hybrid drive system component such as the engine, the motor, and the gearbox. 48V hybrid drive systems adopt parallel hybrid architecture mostly, and parallel hybrid architectures are generally divided into P0~P4 according to the location of the motor (Figure 1). And many studies have been done on the CO2 reduction effect and cost efficiency for each configuration. (Dr. Ing. Olivier COPPIN 2016; Ran Bao and Victor Avila 2017; Thomas Eckenfels and Florian Kolb 2018)

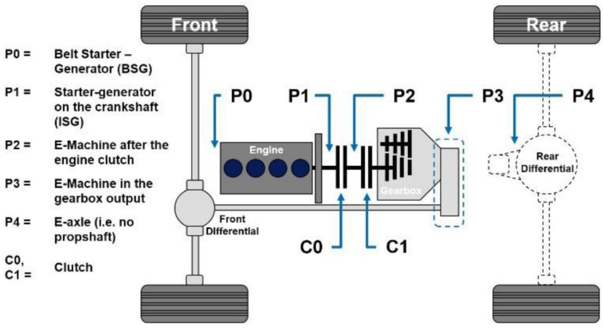

Figure 1: P0~P4 Architecture

However recently, there are the cases composing a 48V hybrid system including not only one motor but also two motor or a 48V electric supercharger, and there is still a lack of research on which architecture is optimal when these components are considered in 48V hybrid system configuration.

The performance of a hybrid system is evaluated with fuel economy mostly. But a hybrid system has been being adapted to various vehicle segments, and since a consumer's expectation is different by vehicle segments, it is needed that evaluating vehicle with performance

other than fuel economy. As related research, Kapadia (2017) compared P2 parallel hybrid architecture and input split hybrid architecture in terms of not only fuel economy but also drivability, launch, power, towing performance and packaging, etc.
Therefore, in this paper, we derived an optimal 48V hybrid system architecture according to fuel economy and performance index when one or two 48V motor and 48V electric supercharger are considered. To do this, we explored 48V hybrid system architecture manually when one or two 48V motors, 48V electric supercharger are considered, and we derived an optimal architecture through *Dynamic programming*. In this case, the cost function of *Dynamic programming* was modified to derive optimal architecture for fuel economy and performance index. Here, the performance index is the index which can evaluate hybrid system performance other than fuel economy, and in this paper, we defined an electric auxiliary load assist ability and drive power reserve as a performance index.

2. EXPLORATION TARGET HYBRID DRIVE ARCHITECTURE

When considering one motor, a 48V hybrid system architecture which can be derived is like Figure 1. In this case, since P0 and P1 architectures have lower fuel economy than P2, P3, and P4 generally, we select P2, P3, and P4 architecture as exploration target hybrid drive architecture having one motor.
And we select the exploration target hybrid drive architecture having two motors like Figure 2. In the figure, the P0D architecture is the architecture that can operate mechanical auxiliary load (ex. water pump, air-conditioner compressor) independently by separating the mechanical auxiliary load from the engine according to the situation. And the motor location is the same as P0 architecture. Since P0D has little higher fuel economy than P0 generally, which is not suggested in this paper, we select P0D architecture instead of P0 architecture for exploration.
Therefore, we select 10 exploration target 48V hybrid drive architecture like below according to motor location and the number of motors.

1. Using one motor: P2, P3, P4
2. Using two motor: P0D +P2, P0D+P3, P0D+P4
   P1 +P2, P1+P3, P1+P4
   P2+P4

But, above 10 architecture doesn't consider a 48V electric supercharger. Therefore finally, we select a total 20 exploration target 48V hybrid drive system architecture by adding 10 architecture having a 48V electric supercharger.
Table 1 below is the specification of the hybrid drive system main components. As we can see in the table, the motor power when using two motors is half of the power when using one motor.

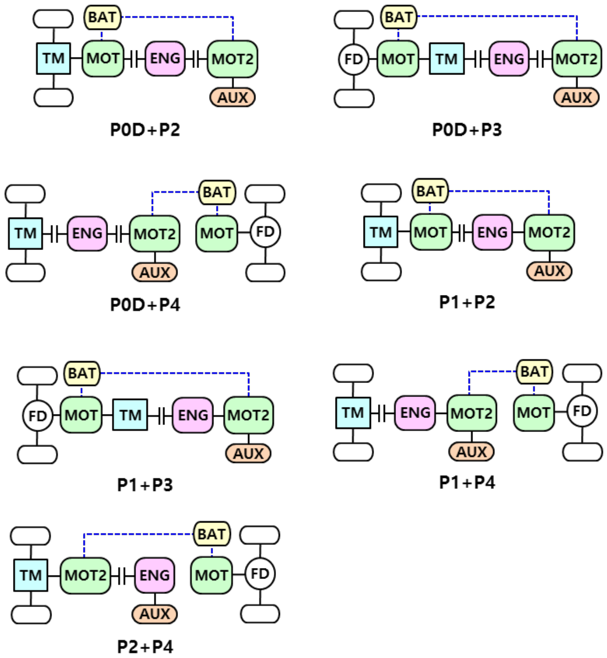

Figure 2: 48V Hybrid Drive System Architecture with Two Motor

Table 1: Specification of Vehicle Component

Component	Specification
Engine	1500 [cc] Gasoline Engine
Motor	10 [kW] PMSM (when using one motor) 5 [kW] PMSM (when using two motor)
Electric Supercharger	5 [kW] PMSM
Battery	48 [V] / 20 [Ah] Lithium-Ion

3. MODEL FOR DYNAMIC PROGRAMMING

We used *Dynamic Programming (DP)* to compare each exploration target hybrid drive system architecture. *DP* is a method of global optimization strategies that find optimal solutions to optimal control problems based on Bellman's principle of optimality. For the hybrid drive system, *DP* is mainly used to analyze the optimal fuel economy results by investigating all possible paths of the vehicle system in a given driving cycle in advance.
Therefore, the *DP* results for any hybrid system architecture can be said to be the optimal performance of the architecture. So, we carry out *DP* simulation about each exploration target hybrid drive architecture and derives optimal architecture by comparing *DP* results.

3.1. Dynamic programming with dpm.m function

In this paper, we use Matlab function dpm.m for *DP*. dpm.m is a *DP* algorithm introduced by Olle Sundström and Lino Guzzella (2009) to solve the general optimization problem. To solve the optimal control problem using the dpm.m function, the user must define the Main.m function and the Model function.m function. The Main.m function sets the range and grid of control

Proc. of the Int. Conference on Modeling and Applied Simulation 2019,
ISBN 978-88-85741-29-4; Bruzzone, De Felice, Dias, Massei and Solis, Eds.

input, state for *DP* and executes dpm.m. Model function.m uses the given inputs to calculate the cost and the state of the next step and returns these values to dpm.m. In this paper, the model function is the vehicle model that calculates the fuel consumption and the SOC variation according to the power distribution ratio, the electric supercharger speed, and transmission gear stage.

3.2. Main.m function setting

As mentioned in Section 3.1, we need the Main.m function and the Model function.m to use dpm.m. This section introduces the settings for the Main.m function. First, we define the control input as below.

1. u_1 : Power distribution ratio for the first motor
2. u_2 : 48V electric supercharger speed
3. u_3 : Gear shift command
4. u_4 : Decoupler on/off command
5. u_5 : Power distribution ratio for the second motor

The decoupler on/off command u_4 is applied to the architecture considering P0D motor, the Power distribution ratio for the second motor u_5 is applied to the architecture considering two motors. The activated control inputs according to architecture is like Table 2.

Table 2: Control Input Setting according to Hybrid Drive System Architecture (O: Use, -: Not use)

Architecture	u_1	u_2	u_3	u_4	u_5
P2	O	O	O	-	-
P3	O	O	O	-	-
P4	O	O	O	-	-
P0D+P2	O	O	O	O	O
P0D+P3	O	O	O	O	O
P0D+P4	O	O	O	O	O
P1+P2	O	O	O	-	O
P1+P3	O	O	O	-	O
P1+P4	O	O	O	-	O
P2+P4	O	O	O	-	O

The mathematical equation of each control input is defined as follows.

First, u_1 and u_5 are defined like Table 3. In the equations below, $\gamma_{ply}, \gamma_{TM}$ is the gear ratio of engine pulley and transmission respectively, $T_{m,i}$ is the motor torque, $T_{tot,i}$ is the vehicle total desired torque (i=2 for P2, 3 for P3, 0D3 for P0D+P3 etc.). And $T_{tot\_f,j}$ is the value of vehicle total desired torque minus P4 motor torque in the architecture having P4 motor. (j=0D4, 14, 24). As we can see in the table, u_1 determines the power distribution of motor which is located relatively far from the engine, u_5 determines the power distribution of the motor which is located relatively close to the engine.

Table 3: Equation of Control Input u_1, u_5

Architecture	u_1	u_5
P2	$T_{m,2}/T_{tot,2}$	-
P3	$T_{m,3}/T_{tot,3}$	-
P4	$T_{m,4}/T_{tot,4}$	-
P0D+P2	$T_{m,2}/T_{tot,0D2}$	$\gamma_{ply}T_{m,0D}/T_{tot,0D2}$
P0D+P3	$T_{m,3}/T_{tot,0D3}$	$\gamma_{TM}\gamma_{ply}T_{m,0D}/T_{tot,0D3}$
P0D+P4	$T_{m,4}/T_{tot,0D4}$	$\gamma_{TM}\gamma_{ply}T_{m,0D}/T_{tot\_f,0D4}$
P1+P2	$T_{m,2}/T_{tot,12}$	$T_{m,1}/T_{tot,12}$
P1+P3	$T_{m,3}/T_{tot,13}$	$\gamma_{TM}T_{m,1}/T_{tot,13}$
P1+P4	$T_{m,4}/T_{tot,14}$	$\gamma_{TM}T_{m,1}/T_{tot\_f,14}$
P2+P4	$T_{m,4}/T_{tot,24}$	$\gamma_{TM}T_{m,2}/T_{tot\_f,24}$

u_3, u_4 are defined like Equation (1), (2) respectively. In Equation (2), Decoupler open means the case that mechanical auxiliary load is separated from an engine, and Decoupler close means the case that mechanical auxiliary load is connected to an engine.

$$u_3 = \begin{cases} 1 & (Upshift) \\ 0 & (No\ shift) \\ -1 & (Downshift) \end{cases} \quad (1)$$

$$u_4 = \begin{cases} 1 & (Decoupler\ open) \\ 0 & (Decoupler\ close) \end{cases} \quad (2)$$

The range and grid of each control input are like Table 4.

Table 4: Range and Grid of Control Input

Control Input	Range	Grid points	Unit
u_1	-1 ~ 1	21	-
u_2	0 ~ 143,000	21	RPM
u_3	-1 ~ 1	3	-
u_4	0 ~ 1	2	-
u_5	-1 ~ 1	21	-

We define states as 48V battery SOC, an engine on/off state, and gear stage of transmission. The range and grid of each state are like Table 5.

Table 5: Range and Grid of State

Control Input	Range	Grid points
SOC	0.3 ~ 0.9	21
Engine On/Off	0 ~ 1	2
Gear Stage	1 ~ 6	6

3.3. Model function.m setting

This section introduces the Model function.m for *DP*. As mentioned above, the model function in this paper is a vehicle model, and the model used in this study is basically the same as the model which was used in the study last year (Ji Y. and Park J. 2018). Therefore, in this paper, we only describe the values which are defined differently from the last year's study depending on the exploration target hybrid system architecture. The values that are defined differently by architecture are vehicle total desired torque, motor torque, cost function.

3.3.1. Total desired torque determination

The vehicle model used in last year's study is P0 architecture. So, the vehicle total desired torque is calculated at the engine crankshaft. In this paper, we define the calculation location of vehicle total desired torque according to architecture, for the convenience of calculation, like Figure 3.

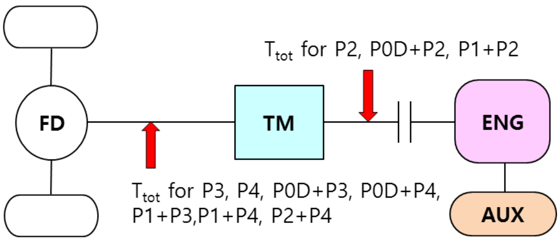

Figure 3: Total Desired Torque Calculation Locations according to Hybrid Drive System Architecture

The vehicle total desired torque according to architecture is calculated as Equation (3) ~ (9). We considered the efficiency of the transmission in a real simulation, but not present in this paper to simplify equation representation. In the equation below, T_{e0} is drive resistance torque of the engine, T_{wp} is load torque of the mechanical auxiliary load, $T_{m0,i}$ (i=2 for P2, 3 for P3, 0D3 for P0D+P3, etc.) is the drive resistance torque of the motor, and γ_{fd} is the gear ratio of the final drive gear. Here, T_{e0} and T_{wp} are calculated at the transmission input shaft. Therefore, for the architecture which calculates vehicle total desired torque at the transmission output shaft, we should calculate these values considering the transmission gear ratio. And since $T_{m0,i}$ is calculated at motor shaft, we should calculate the drive resistance torque of the motor considering the transmission gear ratio or motor location when calculating vehicle total desired torque. In the equation below, T_{e0_diff}, T_{m0,i_diff}, T_{wp_diff} are drive resistance torque of the engine and motor considering the transmission gear ratio, mechanical auxiliary load torque considering the transmission gear ratio respectively.

1. P2

$$T_{tot,2} = \begin{cases} T_{e0} + T_{wp} + T_{m0,2} + \dfrac{T_v}{\gamma_{TM}\gamma_{fd}} & (u_1 \neq 1) \\ T_{m0,2} + \dfrac{T_v}{\gamma_{TM}\gamma_{fd}} & (u_1 = 1) \end{cases} \quad (3)$$

2. P3, P4 ($k = 3,4$)

$$T_{tot,k} = \begin{cases} T_{e0\_diff} + T_{wp\_diff} + T_{m0,k} + \dfrac{T_v}{\gamma_{fd}} & (u_1 \neq 1) \\ T_{m0,k} + \dfrac{T_v}{\gamma_{fd}} & (u_1 = 1) \end{cases} \quad (4)$$

3. P0D+P2

$$T_{tot,0D2} = \begin{cases} T_{e0} + T_{wp} + T_{m0,2} + T_{m0,0D}\gamma_{ply} + \dfrac{T_v}{\gamma_{TM}\gamma_{fd}} & \{(u_1 \neq 1)\,\&\,(u_4 \neq 1)\} \\ T_{e0} + T_{m0,1} + \dfrac{T_v}{\gamma_{TM}\gamma_{fd}} & \{(u_1 \neq 1)\,\&\,(u_4 = 1)\} \\ T_{m0,1} + \dfrac{T_v}{\gamma_{TM}\gamma_{fd}} & \{(u_1 = 1)\} \end{cases}$$

(5)

4. P0D+P3, P0D+P4 ($k = 3,4$)

$$T_{tot,0Dk} = \begin{cases} T_{e0\_diff} + T_{wp\_diff} + T_{m0,k} + T_{m0,0D\_diff} + \dfrac{T_v}{\gamma_{fd}} & \{(u_1 \neq 1)\,\&\,(u_4 \neq 1)\} \\ T_{e0\_diff} + T_{m0,k} + \dfrac{T_v}{\gamma_{fd}} & \{(u_1 \neq 1)\,\&\,(u_4 = 1)\} \\ T_{m0,k} + \dfrac{T_v}{\gamma_{fd}} & \{(u_1 = 1)\} \end{cases}$$

(6)

5. P1+P2

$$T_{tot,12} = \begin{cases} T_{e0} + T_{wp} + T_{m0,1} + T_{m0,2} + \dfrac{T_v}{\gamma_{TM}\gamma_{fd}} & (u_1 \neq 1) \\ T_{m0,1} + \dfrac{T_v}{\gamma_{TM}\gamma_{fd}} & (u_1 = 1) \end{cases} \quad (7)$$

6. P1+P3, P1+P4 ($k = 3,4$)

$$T_{tot,1k} = \begin{cases} T_{e0\_diff} + T_{wp\_diff} + T_{m0,k} + T_{m0,1\_diff} + \dfrac{T_v}{\gamma_{fd}} & (u_1 \neq 1) \\ T_{m0,k} + \dfrac{T_v}{\gamma_{fd}} & (u_1 = 1) \end{cases}$$

(8)

7. P2+P4

$$T_{tot,24} = \begin{cases} T_{e0\_diff} + T_{wp\_diff} + T_{m0,4} + T_{m0,2\_diff} + \dfrac{T_v}{\gamma_{fd}} & (u_1 + u_5 \neq 1) \\ T_{m0,4} + T_{m0,2} + \dfrac{T_v}{\gamma_{fd}} & (u_1 + u_5 = 1) \end{cases}$$

(9)

3.3.2. Motor torque determination by u_1 (First motor)

Table 6 shows the motor of which torque is determined by control input u_1, according to the architecture, and we let say this motor as the first motor from now on. The torque of the motor is calculated as Equation (10). In the Equation (10), $T_{m,i}$ is the torque of the motor of which torque is determined by u_1 for each architecture, and $T_{tot,k}$ is the vehicle total desired torque for each architecture.

Table 6: The Motor of which Torque is determined by Control Input u_1

Architecture		Architecture	
P2	P2	P0D+P4	P4
P3	P3	P1+P2	P2
P4	P4	P1+P3	P3
P0D+P2	P2	P1+P4	P4
P0D+P3	P3	P2+P4	P4

$$T_{m,i} = u_1 T_{tot,k} \;\; (i = 2,3,4, k = 2,3,4,0D2,0D3,.....) \quad (10)$$

3.3.3. Motor torque determination by u_5 (Second motor)

Table 7 shows the motor of which torque is determined by control input u_5, according to the architecture, and we let say this motor as the second motor from now on.

Table 7: The Motor of which Torque is determined by Control Input u_5

Architecture		Architecture	
P0D+P2	P0D	P1+P2	P1
P0D+P3		P1+P3	
P0D+P4		P1+P4	
		P2+P4	

If the case of $u_1 = 1$, since the vehicle is propelled by the first motor only, the second motor doesn't generate any torque. Therefore, the second motor torque is determined differently by u_1. And in the case of P0D motor, the torque of the motor is differed by decoupler state. With consideration of these characteristics, the motor torque is determined like Equation (11) ~ (16), according to the architecture. In Equation (13), C_{eff} is the efficiency of delivered driving power, and η_{trans} has the value between 0 and 1. This is the parameter for reflecting power distribution characteristic when motors are located at both front and rear wheel. For example, when the motors of the front and rear wheel all propel the vehicle or all brake the vehicle, each drive power is delivered to ground directly. But when the motor of front wheel propels the vehicle and the motor of rear wheel generate power using front wheel power, the front wheel power is delivered rear wheel motor through the ground. So, in that case, we should consider the efficiency of the delivered drive power. For reflecting these characteristics, we use C_{eff} when architecture has a P4 motor.

1. P0D+P2

$$T_{m,0D} = \begin{cases} u_5 \dfrac{T_{tot,0D2}}{\gamma_{ply}} & \{(u_4 \neq 1) \,\&\, (u_1 \neq 1)\} \\ 0 & \{(u_4 \neq 1) \,\&\, (u_1 = 1)\} \\ T_{m0m0D} + \dfrac{T_{wp}}{\gamma_{ply}} & \{(u_4 = 1)\} \end{cases}$$

(11)

2. P0D+P3

$$T_{m,0D} = \begin{cases} u_5 \dfrac{T_{tot,0D3}}{\gamma_{TM}\gamma_{ply}} & \{(u_4 \neq 1) \& (u_1 \neq 1)\} \\ 0 & \{(u_4 \neq 1) \& (u_1 = 1)\} \\ T_{m0,0D} + \dfrac{T_{wp}}{\gamma_{ply}} & \{(u_4 = 1)\} \end{cases} \tag{12}$$

3. P0D+P4

$$T_{tot\_f,0D4} = T_{tot,0D4} - C_{eff} T_{m,4}$$

$$C_{eff} = \begin{cases} 1/\eta_{trans} & \{(T_{tot,0D4} \geq 0) \& (u_1 T_{m,4} \leq 0)\} \\ 1 & (otherwise) \end{cases}$$

$$T_{m,0D} = \begin{cases} u_5 \dfrac{T_{tot\_f,0D4}}{\gamma_{TM}\gamma_{ply}} & \{(u_4 \neq 1) \& (u_1 \neq 1)\} \\ 0 & \{(u_4 \neq 1) \& (u_1 = 1)\} \\ T_{m0,0D} + \dfrac{T_{wp}}{\gamma_{ply}} & \{(u_4 = 1)\} \end{cases} \tag{13}$$

4. P1+P2

$$T_{m,1} = \begin{cases} u_5 T_{tot,12} & (u_1 \neq 1) \\ 0 & (u_1 = 1) \end{cases} \tag{14}$$

5. P1+P3

$$T_{m,1} = \begin{cases} u_5 \dfrac{T_{tot,13}}{\gamma_{TM}} & (u_1 \neq 1) \\ 0 & (u_1 = 1) \end{cases} \tag{15}$$

6. P1+P4, P2+P4

$$T_{m,1} = \begin{cases} u_5 \dfrac{T_{tot\_f,14}}{\gamma_{TM}} & (u_1 \neq 1) \\ 0 & (u_1 = 1) \end{cases} \tag{16}$$

3.3.4. Cost

The dpm.m function sum the all cost per step to determine the optimal path. In this paper, the cost is defined by performance index differently.

The cost for fuel economy and additional performance index, electric auxiliary load assist ability is fuel consumption per step time like Equation (17). Therefore, The *DP* for fuel economy and electric auxiliary assist ability will find the optimal path which minimizes fuel consumption.

The cost for drive power reserve is like Equation (18). In the equation, Δm_{fuel} is fuel consumption per step time, k_{pwr} is the coefficient for drive power reserve, $P_{e,max}, P_e$ are the engine maximum power and current power respectively, ω_e , $\omega_{e\text{-}SC}$ are the speed of the engine and 48V electric supercharger respectively, H_{LHV} is a low-heating value of fuel, T_s is step time. And we can see that the second term of Equation (18) has the same unit with fuel consumption. By this term, the engine drive power reserve (The engine maximum power – current power) became larger, the cost became smaller. So, The *DP* for drive power reserve will find the optimal path which maximizes drive power reserve and minimizes fuel consumption.

$$J = \Delta m_{fuel} \tag{17}$$

$$J = \Delta m_{fuel} - k_{pwr} \frac{P_{e,max}(\omega_e, \omega_{e-SC}) - P_e}{H_{LHV}} T_s \tag{18}$$

4. DYNAMIC PROGRAMMING RESULT

4.1. Test scenario

In order to compare performance for each architecture, we carry out *DP* simulation for FTP-75 which is one of the driving cycles that used for evaluating fuel economy of a hybrid electric vehicle generally. The speed profile reference of a vehicle is like Figure 4.

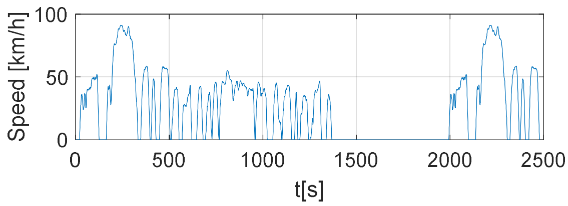

Figure 4: The Speed Profile of FTP-75 Cycle

4.2. Performance index

In this paper, we evaluate hybrid drive system architecture through fuel economy, electric auxiliary load assist ability, and drive power reserve. The index for evaluating each performance is calculated like below respectively.

4.2.1. Fuel economy

We calculate fuel economy like Equation (19) that calculate fuel economy by the total fuel consumption versus total travel distance of the vehicle. In this case, the cost of Model function.m is Equation (17). In the Equation (19), FE is fuel economy of the vehicle,

$Dist_{tot}$ is total travel distance of the vehicle when driving FTP-75 cycle, F_{base} is total fuel consumption when we use cost as Equation (17).

$$FE = \frac{Dist_{tot}}{\sum \Delta m_{fuel}}, \quad F_{base} = \sum \Delta m_{fuel} \qquad (19)$$

4.2.2. Electric auxiliary load assist ability performance index

For the case of electric auxiliary load assist ability, the cost of the Model function.m is Equation (17) as the case of fuel economy also. We evaluate the electric auxiliary load assist ability by fuel consumption difference between when an additional electric auxiliary load is applied and when is not applied. If the difference is not large, we can say that the architecture has high electric auxiliary load assist ability because it has a low reduction of fuel economy by an additional electric auxiliary load.

In order to compare performance according to an additional electric auxiliary load size, we apply two kinds of additional loads, 300[W] and 1000[W]. The electric auxiliary load assist ability is defined as Equation (20). In Equation (20), $F_{FE,base}$ is the fuel consumption when an additional electric auxiliary load is not applied, $F_{FE,accelec}$ is the fuel consumption when an additional electric auxiliary load, $P_{elec,add}$, is applied by 300[W] or 1000[W].

$$\begin{aligned} F_{elec,acc} &= F_{FE,accelec} - F_{FE,base} \\ F_{FE,base} &= \sum \Delta m_{fuel} \, (@ P_{elec,add} = 0) \\ F_{FE,accelec} &= \sum \Delta m_{fuel} (@ P_{elec,add} = 300 \, or \, 1000) \end{aligned} \qquad (20)$$

4.2.3. Drive power reserve performance index

We evaluate the performance of the drive power reserve as the total summation of drive power reserve per step time when we set the cost of Model function.m as Equation (18). In other words, the drive power reserve performance $F_{pwr,rsv}$ is defined as Equation (21).

$$F_{pwr,rsv} = \sum \frac{P_{e,max}(\omega_e, \omega_{e-SC}) - P_e}{H_{LHV}} T_s \qquad (21)$$

4.2.4. Comprehensive performance index

We defined the performance of electric auxiliary load assist ability and drive power reserve as Equation (20), (21). We defined each performance index as the concept of fuel consumption, and the reason for this is to solve the scaling problem when calculating the comprehensive performance index. The comprehensive performance index (F_{total}) that integrates all performance index which is described earlier is Equation (22). In Equation (22), α_0, α_1, and α_2 are the weight of each performance index respectively, and a user can adjust the weight when deriving optimal hybrid system architecture, according to what performance is more important. For example, If a user wants the optimal architecture which has higher electric auxiliary load assist ability than fuel economy and the drive power reserve, the user can set the weight as $\alpha_0 = 0.1$, $\alpha_1 = 1$, $\alpha_2 = 0.1$. Each weight has a positive value.

$$F_{total} = \alpha_0 F_{base} + \alpha_1 F_{elec,acc} - \alpha_2 F_{pwr,rsv} \qquad (22)$$

4.3. Comparison of fuel economy

The fuel economy results for each architecture obtained by *DP* simulation (FTP-75) is like Figure 5. In this case, we set the cost of Model function.m as Equation (17). We can see P2 architecture have the best fuel economy. The reason for this may be that the motor of P2 architecture can operate at a higher efficiency operating point than other architecture by optimizing the gear stage. And for all architectures, we can see that they have higher fuel economy when a 48V electric supercharger is applied. Therefore, we can conclude that the optimal architecture for fuel economy is P2 with e-SC (48V electric supercharger) architecture.

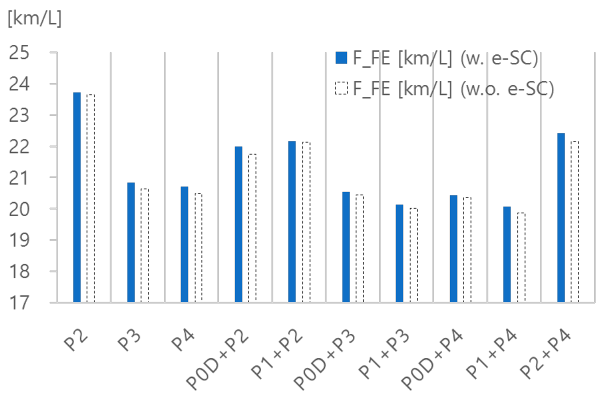

Figure 5: Comparison of FE

4.4. Comparison of electric accessory load assist ability

The electric auxiliary load assist ability for each architecture obtained by *DP* simulation (FTP-75) is like Figure 6, 7. In this case, we set the cost of Model function.m as Equation (17) and apply additional electric auxiliary load. Figure 6 and 7 are the case when an additional electric auxiliary load is 300[W] and 1000[W] respectively. The electric auxiliary load assist ability performance index has a low value when the electric auxiliary load assist ability is high. For both cases that additional electric auxiliary loads are 300[W] and 1000[W] respectively, we can see that the P0D+P2 with e-SC architecture has the best electric auxiliary load assist ability. Therefore, we can conclude that the optimal architecture for the electric auxiliary load assist ability is P0D+P2 with e-SC architecture.

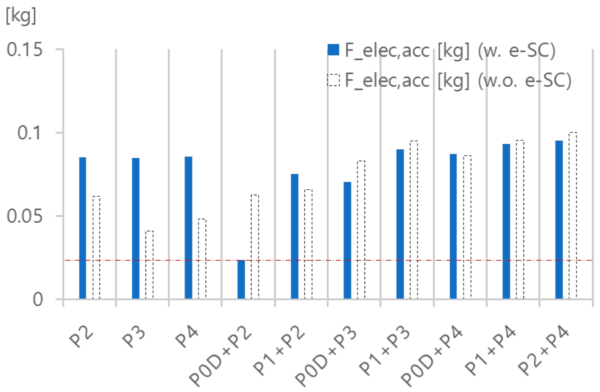

Figure 6: Comparison of $F_{elec,acc}$ **(**$P_{elec,add} = 300$**)**

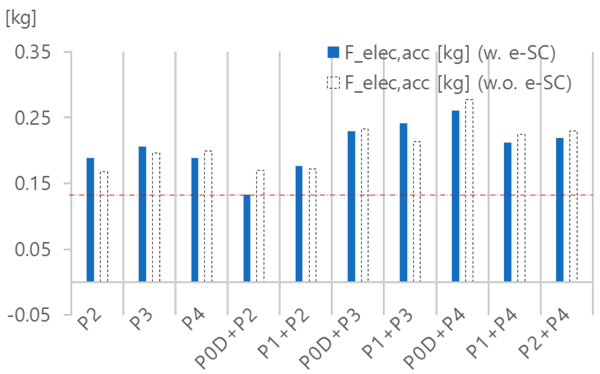

Figure 7: Comparison of $F_{elec,acc}$ **(**$P_{elec,add} = 1000$**)**

4.5. Comparison of drive power reserve

The drive power reserve for each architecture obtained by *DP* simulation (FTP-75) is like Figure 8. In this case, we set the cost of Model function.m as Equation (18). The drive power reserve performance index has a high value when the drive power reserve is high. So, we can see that the P0D+P2 without e-SC architecture has the best drive power reserve. Therefore, we can conclude that the optimal architecture for the drive power reserve is P0D+P2 without e-SC architecture.

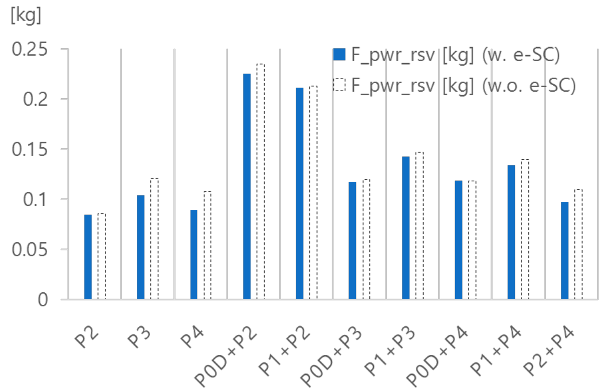

Figure 8: Comparison of $F_{pwr,rsv}$

4.6. Comparison of Comprehensive Performance Index

The comprehensive performance index is differed by weight value, α_0, α_1, α_2. In this paper, we show one examples by setting α_0, α_1, α_2 to 1 all. In other words, the optimal architecture derived from these weight values will be the architecture that has proper fuel economy, electric auxiliary load assist ability and drive power reserve. We calculate the comprehensive performance index for each architecture using performance indices which are calculated in previous sections, and the results are like Figure 9, 10. For both cases of additional electric auxiliary load are 300[W] and 1000[W] respectively, we can see that the P0D+P2 without e-SC architecture has the lowest comprehensive performance index. Therefore, we can conclude that the optimal architecture for the comprehensive performance index is P0D+P2 without e-SC architecture.

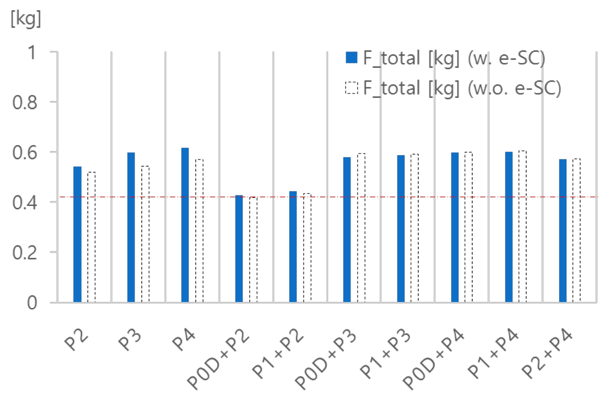

Figure 9: Comparison of F_{total} **(**$P_{elec,add} = 300$**)**

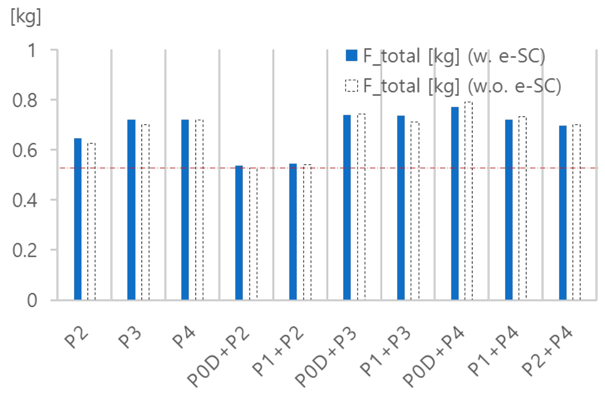

Figure 10: Comparison of F_{total} ($P_{elec,add} = 1000$)

4.7. Ranking by Each Performance Index

Table 8 and 9 are the ranking of the performance indices which are calculated in previous sections. The ranking is low when performance is high. In other words, FE , $F_{pwr,rsv}$ are ordered in which the performance indices are high, and $P_{elec,add}$ are ordered in which the performance indices are low.

In the case of fuel economy, we can see that the architectures having the P2 motor tend to have a high fuel economy. And In the case of the drive power reserve, we can see that the architecture having the motor connected directly to the engine crankshaft (P0D, P1) tend to have a high drive power reserve. In the case of the electric auxiliary load assist ability, we can't find a clear trend when an additional electric auxiliary load is 300[W]. But when an additional electric auxiliary load is 1000[W], we can see that the architecture having both P2 motor and the motor connected directly to the engine crankshaft tend to have a high electric auxiliary load assist ability.

Therefore, taking above analysis together, we can conclude that we should select the P2 architecture when fuel economy is the most important, and select the architecture having crankshaft direct connection motor and P2 motor when electric auxiliary load assist ability or drive power reserve is most important.

Table 8: Ranking by FE and $F_{pwr,rsv}$

Rank	FE		$F_{pwr,rsv}$	
	Architecture	48V e-SC	Architecture	48V e-SC
1	P2	O	P0D+P2	-
2	P2	-	P0D+P2	O
3	P2+P4	O	P1+P2	-
4	P1+P2	O	P1+P2	O
5	P2+P4	-	P1+P3	-
6	P1+P2	-	P1+P3	O
7	P0D+P2	O	P1+P4	-
8	P0D+P2	-	P1+P4	O
9	P3	O	P3	-
10	P4	O	P0D+P3	-
11	P3	-	P0D+P4	-
12	P0D+P3	O	P0D+P4	O
13	P4	-	P0D+P3	O
14	P0D+P4	O	P2+P4	-
15	P0D+P3	-	P4	-
16	P0D+P4	-	P3	O
17	P1+P3	O	P2+P4	O
18	P1+P4	O	P4	O
19	P1+P3	-	P2	-
20	P1+P4	-	P2	O

Table 9: Ranking by $P_{elec,add}$

Rank	$F_{elec,acc}$ ($P_{elec,add} = 300$)		$F_{elec,acc}$ ($P_{elec,add} = 1000$)	
	Architecture	48V e-SC	Architecture	48V e-SC
1	P0D+P2	O	P0D+P2	O
2	P3	-	P2	-
3	P4	-	P0D+P2	-
4	P2	-	P1+P2	-
5	P0D+P2	-	P1+P2	O
6	P1+P2	-	P2	O
7	P0D+P3	O	P4	O
8	P1+P2	O	P3	-
9	P0D+P3	-	P4	-
10	P3	O	P3	O
11	P2	O	P1+P4	O
12	P4	O	P1+P3	-
13	P0D+P4	-	P2+P4	O
14	P0D+P4	O	P1+P4	-
15	P1+P3	O	P0D+P3	O
16	P1+P4	O	P2+P4	-
17	P1+P3	-	P0D+P3	-
18	P2+P4	O	P1+P3	O
19	P1+P4	-	P0D+P4	O
20	P2+P4	-	P0D+P4	-

5. CONCLUSION

In this paper, we selected exploration target 48V hybrid drive architecture by exploring possible 48V hybrid drive system manually and compared the performance of each architecture through *DP* simulation. When comparing the performance of the hybrid system, we used not only fuel economy but also electric auxiliary load assist ability and drive power reserve. Here, we developed performance indices for electric auxiliary load assist ability and drive power reserve in order to compare performance. And the performance indices have a unit of fuel consumption in order to solve the problem scaling when calculating comprehensive performance index. As results, we found that P2 is the optimal architecture for fuel economy, and the architecture having crankshaft direct connection motor (P0D, P1) and P2 motor is the optimal architecture for electric auxiliary load assist ability or drive power reserve.

We considered an engine only when calculating drive power reserve performance index. But a hybrid electric vehicle has not only an engine but also a motor for driving. Therefore, in future work, if we consider a drive power reserve of an engine and a motor together, the drive power reserve performance is expected to be evaluated more accurately.

ACKNOWLEDGMENTS

This work was supported by the Industrial Strategic Technology Development Program (10076437, Development of hybrid drive topology exploration and control technology for fuel economy optimization of 48V mild HEVs) funded By the Ministry of Trade, Industry & Energy(MOTIE, Korea).

REFERENCES

Andreas Baumgardt, Dieter Gerling, 2015a. 48V Recuperation Storage Based on Supercaps for Automotive Application, EVS28 International Electric Vehicle Symposium and Exhibition, May 3-6, KINTEX (Korea).

Andreas Baumgardt, Dieter Gerling, 2015b. 48V Recuperation Storage Including Stabilizing 12V Tap for HEVs, 2015 IEEE Transportation Electrification Conference and Expo (ITEC), June 14-17, Dearborn (Michigan, USA).

Anthony Rick, Brain Sisk, 2015. A Simulation Based Analysis of 12V and 48V Microhybrid Systems Across Vehicle Segments and Drive Cycle, SAE 2015 World Congress & Exhibition, April 21-23. Detroit (Michigan, USA).

Dr. Ing. Olivier COPPIN, 2016. Valeo Presentation – From 12 plus 12V to 48V. Available from: https://48v-vehicles.iqpc.de/downloads/valeo-presentation-from-12-plus-12v-to-48v [accessed 5 March 2019]

Ji Y., Park J, Lee H., 2018. A study on operating characteristics of a 48V electric supercharger and P0 configuration motor for fuel economy improvement. MAS 2018, September 17, 39-47.

Junyong Park, Taeho Park, Hyeongcheol Lee, 2017. An optimization of power distribution considering supercharging characteristic for electric supercharger applied 48V mild hybrid vehicle, KSAE 2017 Annual Autumn Conference & Exhibition, pp.1328-1333. November 15-18, Yeosu (Jeollanam-do, South Korea).

Kapadia J., Kok D., Jennings M., Kuang M., Masterson B., Isaacs R., Dona A., Wagner C., and Gee T., 2017. Powersplit or Parallel - Selecting the Right Hybrid Architecture. SAE International Journal of Alternative Powertrains, 6.

Malte Kuypers, 2014. Application of 48 Volt for Mild Hybrid Vehicles and High Power Load, SAE 2014 World Congress & Exhibition, April 1, Detroit (Michigan, USA).

Mark Schudeleit, Christian Sieg, Ferit Kücükay, 2015. The Potential of 48V HEV in Real Driving, International Scholarly and Scientific Research & Innovation Vol: 9 No: 10, 1719-1728.

Olle Sundstrom, Lino Guzzella, 2009. A Generic Dynamic Programming Matlab Function, 18th IEEE International Conference on Control Applications Part of 2009 IEEE Multi-conference on Systems and Control Saint Petersburg, July 8-10, St. Petersburg (Russia).

Ran Bao, Victor Avila, James Baxter, 2017. Effect of 48V Mild Hybrid System Layout on Powertrain System Efficiency and Its Potential of Fuel Economy Improvement, WCX™ 17: SAE World Congress Experience, April 4-6, Detroit (Michigan, USA).

Thomas Eckenfels, Florian Kolb, Steffen Lehmann, Waldemar Neugebauer, Manel Calero, 2018. 48V Hybridization, A Smart Upgrade for the Powertrain. Available from: http://schaeffler-events.com/symposium/lecture/h3/index.html [accessed 6 July 2018]

Zifan Liu, Andrej Ivanco, and Zoran S. Filipi, 2016. Impact of Real-World Driving and Driver Aggressiveness on Fuel Consumption of 48V Mild Hybrid Vehicle, SAE International, April 5, 249-258.